Investigation of the Non-Equilibrium Structures in Inert Hypersonic Shock Waves with the Twenty-Moment Equations

Ethan D. Rice[1] Stefano Boccelli[2] James G. McDonald[1]

[1]Department of Mechanical Engineering
University of Ottawa

[2]Goddard Space Flight Center
NASA

36th Thermal and Fluids Analysis Workshop, August 6th 2025

uOttawa

Motivation for Moment Methods

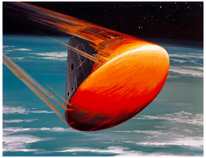

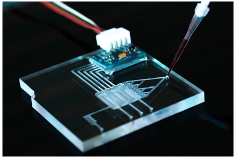

- Sufficiently rarefied gases violate the continuum assumption, and existing models, like the Navier-Stokes Equations, break down

$$\mathrm{Kn} = \frac{\lambda}{L}$$

- For cases such as strong shocks or nanoscale flows, non-equilbrium effects can be important for physically accurate modeling, but are invisible to continuum models

Motivation to Investigate Non-Equilibrium

- Shock structure is not discontinuous, and the thermodynamic temperature doesn't tell the whole story

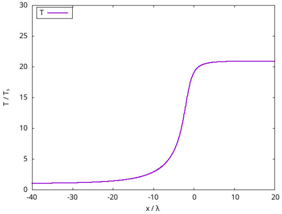

Motivation to Investigate Non-Equilibrium

- Shock structure is not discontinuous, and the thermodynamic temperature doesn't tell the whole story

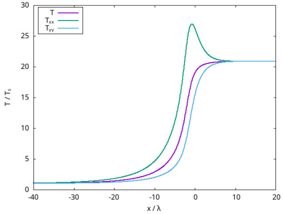

Pre-shock

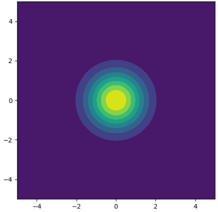

Mid-shock

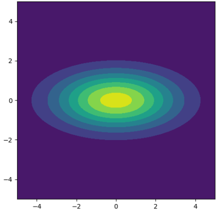

Post-shock

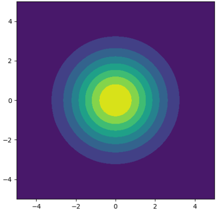

Moment Methods

Advantages with moment methods

- Inherently capture anisotropies, and other non-equilibrium physics like heat fluxes, by modeling gases probabilistically
- Efficient to solve, if you can solve the Euler equations, you can solve a moment method

Moment Methods

Advantages with moment methods

- Inherently capture anisotropies, and other non-equilibrium physics like heat fluxes, by modeling gases probabilistically
- Efficient to solve, if you can solve the Euler equations, you can solve a moment method

Still have some problems

- Ensuring resulting PDEs are robustly hyperbolic has been challenging
- Lots of work on academic one-dimensional models, but extensions to a realistic three-dimensional gas is difficult

Kinetic Theory Background

- Distribution Function:

$$\mathcal{F}\left(x_i, v_i, t\right)$$

- Moments:

$$U_{ij\ldots n} = \iiint_{\infty} m v_i v_j \ldots v_n \mathcal{F} dv_i = \langle m v_i v_j \ldots v_n \mathcal{F} \rangle$$

$$U_0 = \langle m\mathcal{F} \rangle = \rho \qquad U_x = \langle m v_x \mathcal{F} \rangle = \rho u_x \qquad U_{xx} = \left\langle m v_x^2 \mathcal{F} \right\rangle = \rho u_x^2 + P_{xx}$$

- Random Part of Moments with $c_i = v_i - u_i$:

$$P_{xy} = \langle m c_x c_y \mathcal{F} \rangle \qquad Q_{xxy} = \left\langle m c_x^2 c_y \mathcal{F} \right\rangle \qquad R_{xxyz} = \left\langle m c_x^2 c_y c_z \mathcal{F} \right\rangle$$

- High-order Convected Moments:

$$\begin{aligned} U_{ijk} &= \langle m v_i v_j v_k \mathcal{F} \rangle = \langle m \left(u_i + c_i\right)\left(u_j + c_j\right)\left(u_k + c_k\right) \mathcal{F} \rangle \\ &= \langle m \left(u_i u_j u_k + c_i u_j u_k + c_j u_i u_k + c_k u_i u_j + c_i c_j u_k + c_i c_k u_j + c_j c_k u_i + c_i c_j c_k\right) \mathcal{F} \rangle \\ &= \rho u_i u_j u_k + P_{ij} u_k + P_{ik} u_j + P_{jk} u_i + Q_{ijk} \end{aligned}$$

Boltzmann Equation and Maxwell's Equation of Change

- Boltzmann Equation:

$$\frac{\partial \mathcal{F}}{\partial t} + v_i \frac{\partial \mathcal{F}}{\partial x_i} = \frac{\delta \mathcal{F}}{\delta t}$$

- Maxwell's Equation of Change with velocity weight vector $\boldsymbol{w} = [w_1, w_2, ..., w_n]^{\mathsf{T}}$ and BGK collisions:

$$\frac{\partial}{\partial t}\left\langle m\boldsymbol{w}\mathcal{F}\right\rangle + \frac{\partial}{\partial x_i}\left\langle m\boldsymbol{w}v_i\mathcal{F}\right\rangle = \left\langle -m\boldsymbol{w}\frac{\mathcal{F}-\mathcal{M}}{\tau}\right\rangle$$

- Collision frequency can either be constant, or modeled based on the local state

$$\tau = \frac{\mu_{ref}}{p}\left(\frac{T}{T_{ref}}\right)^{\omega}$$

- Written with moment vector $\boldsymbol{U}$, flux vector $\boldsymbol{F}_i$, and source vector $\boldsymbol{S}$:

$$\frac{\partial \boldsymbol{U}}{\partial t} + \frac{\partial \boldsymbol{F}_i}{\partial x_i} = \boldsymbol{S}\left(\boldsymbol{U}\right) \qquad \text{or} \qquad \frac{\partial \boldsymbol{U}}{\partial t} + \frac{\mathrm{d}\boldsymbol{F}_\mathrm{i}}{\mathrm{d}\boldsymbol{U}}\frac{\partial \boldsymbol{U}}{\partial x_i} = \boldsymbol{S}\left(\boldsymbol{U}\right)$$

Euler Equations

- Gases in local thermodynamic equilibirum have a Maxwellian distribution

$$\mathcal{F} = \mathcal{M} = \frac{\rho}{m}\left(\frac{\rho}{2\pi p}\right)^{\frac{3}{2}} \exp\left(\frac{\rho}{2p}(v_i - u_i)(v_i - u_i)\right)$$

- Continuity Equation:

$$\frac{\partial}{\partial t}(\rho) + \frac{\partial}{\partial x_i}(\rho u_i) = 0$$

- Momentum Equation:

$$\frac{\partial}{\partial t}(\rho u_i) + \frac{\partial}{\partial x_j}(\rho u_i u_j + P\delta_{ij}) = 0$$

- Energy Equation:

$$\frac{\partial}{\partial t}(\rho u_i u_i + 3P) + \frac{\partial}{\partial x_j}(\rho u_j u_i u_i + 5P u_j) = 0$$

Existing Non-Equilibirum Models

Get the statistics directly

- Numerically Integrate Kinetic Equations (BGK)
- Direct Simulation Monte Carlo (DSMC)

Existing moment closures by assuming a distribution function

- Grad Hierarchy (Grad, 1949):

$$\mathcal{F} = \left(\alpha_0 H_0(v_i) + \alpha_j H_j(v_i) + \alpha_{jk} H_{jk}(v_i) + \ldots\right) \mathcal{M}$$

- **Maximum Entropy** (Dreyer, 1987, Müller and Ruggeri, 1993, Levermore, 1996):

$$\mathcal{F} = \exp(\boldsymbol{\alpha}^T \boldsymbol{w})$$

- Phi-Divergence (Abdelmalik and van Brummelen, 2015):

$$\mathcal{F} = \mathcal{M}\left(1 + \frac{\boldsymbol{\alpha}^T \boldsymbol{w}}{N}\right)^N$$

New One-Dimensional Closures

- HyQMOM Hierarchy (Fox and Laurent, 2022) and Orthogonal Polynomial Hierarchy (Morin and McDonald 2024) focus on resulting PDEs instead of integrable distribution
- Example of the new hierarchies, 4-moment equations:

$$\frac{\partial}{\partial t}(\rho) + \frac{\partial}{\partial x}(\rho u) = 0$$

$$\frac{\partial}{\partial t}(\rho u) + \frac{\partial}{\partial x}\left(\rho u^2 + p\right) = 0$$

$$\frac{\partial}{\partial t}\left(\rho u^2 + p\right) + \frac{\partial}{\partial x}\left(\rho u^3 + 3pu + q\right) = 0$$

$$\frac{\partial}{\partial t}\left(\rho u^3 + 3pu + q\right) + \frac{\partial}{\partial x}\left(\rho u^4 + 6pu^2 + 4qu + r\right) = 0$$

$$r = 2\frac{q^2}{p} + 3\frac{p^2}{\rho}$$

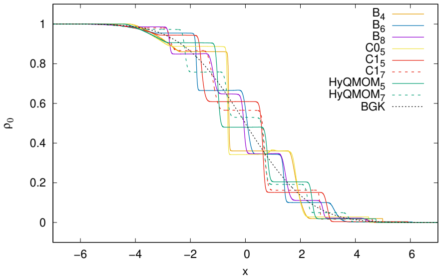

New One-Dimensional Closures

- Flux Jacobians in one dimension of velocity space have the form of a companion matrix:

$$\frac{\mathrm{d}\boldsymbol{F}}{\mathrm{d}\boldsymbol{U}} = \begin{bmatrix} 0 & 1 & 0 & \dots & 0 \\ 0 & 0 & 1 & \dots & 0 \\ \vdots & \vdots & \vdots & \ddots & \vdots \\ 0 & 0 & 0 & \dots & 1 \\ \frac{\partial F_n}{\partial U_0} & \frac{\partial F_n}{\partial U_1} & \frac{\partial F_n}{\partial U_2} & \dots & \frac{\partial F_n}{\partial U_n} \end{bmatrix}$$

- Which have the characteristic polynomial:

$$\det\left(\lambda I - \frac{\partial \boldsymbol{F}_x}{\partial \boldsymbol{U}}\right) = \lambda^n - \frac{\partial F_n}{\partial U_n}\lambda^{n-1} - \dots - \frac{\partial F_n}{\partial U_2}\lambda^2 - \frac{\partial F_n}{\partial U_1}\lambda - \frac{\partial F_n}{\partial U_0} = 0$$

- Extending the mathematical properties of the one-dimensional closures to realistic, three-dimensional gases has proven challenging

10-Moment Equations

- The maximum entropy distribution for a realistic three-dimensional gas with a general pressure tensor P_{ij} has a Gaussian distribution:

$$\mathcal{G} = \frac{1}{m}\left(\frac{\rho}{2\pi}\right)^{\frac{3}{2}}\left(\frac{1}{\det P_{ij}}\right)^{\frac{1}{2}}\exp\left(-\frac{\rho}{2}P_{ij}^{-1}c_i c_j\right)$$

- Continuity Equation:

$$\frac{\partial}{\partial t}(\rho) + \frac{\partial}{\partial x_i}(\rho u_i) = 0$$

- Momentum Equation:

$$\frac{\partial}{\partial t}(\rho u_i) + \frac{\partial}{\partial x_j}(\rho u_i u_j + P_{ij}) = 0$$

- Energy Equation:

$$\frac{\partial}{\partial t}(\rho u_i u_j + P_{ij}) + \frac{\partial}{\partial x_k}(\rho u_i u_j u_k + P_{ij} u_k + P_{ik} u_j + P_{jk} u_i) = \boldsymbol{S}(\boldsymbol{U})$$

10-Moment Closure Structure

- Re-order equations with $\boldsymbol{w} = \left[1, v_x, v_x^2, v_y, v_x v_y, v_z, v_x v_z, v_y^2, v_y v_z, v_z^2\right]^T$ and study the resulting Jacobian in the x-direction

$$\frac{\partial}{\partial t}\begin{bmatrix} \rho \\ \rho u_x \\ \rho u_x^2 + P_{xx} \\ \rho u_y \\ \rho u_x u_y + P_{xy} \\ \rho u_z \\ \rho u_x u_z + P_{xz} \\ \rho u_y^2 + P_{yy} \\ \rho u_y u_z + P_{yz} \\ \rho u_z^2 + P_{zz} \end{bmatrix} + \frac{\partial}{\partial x}\begin{bmatrix} \rho u_x \\ \rho u_x^2 + P_{xx} \\ \rho u_x^3 + 3P_{xx} u_x \\ \rho u_y \\ \rho u_x u_y + P_{xy} \\ \rho u_x^2 u_y + 2P_{xy} u_x + P_{xx} u_y \\ \rho u_z \\ \rho u_x u_z + P_{xz} \\ \rho u_x^2 u_z + 2P_{xz} u_x + P_{xx} u_z \\ \rho u_x u_y^2 + 2P_{xy} u_y + P_{yy} u_x \\ \rho u_x u_y u_z + P_{yz} u_x + P_{xz} u_y + P_{xy} u_z \\ \rho u_x u_z^2 + 2P_{xz} u_z + P_{zz} u_x \end{bmatrix} + \cdots = \boldsymbol{S}$$

10-Moment Flux Jacobian

- Sparse upper allows for some decoupling of the sub-systems

$$
\frac{\partial \boldsymbol{F}_x}{\partial \boldsymbol{U}} = \begin{bmatrix}
0 & 1 & 0 & 0 & 0 & 0 & 0 & 0 & 0 & 0 \\
0 & 0 & 1 & 0 & 0 & 0 & 0 & 0 & 0 & 0 \\
u_x^3 - 3\frac{P_{xx}u_x}{\rho} & -3u_x^2 + 3\frac{P_{xx}}{\rho} & 3u_x & 0 & 0 & 0 & 0 & 0 & 0 & 0 \\
0 & 0 & 0 & 0 & 1 & 0 & 0 & 0 & 0 & 0 \\
u_x^2 u_y - \frac{P_{xx}u_y}{\rho} - \frac{2P_{xy}u_x}{\rho} & -2u_x u_y + \frac{2P_{xy}}{\rho} & u_y & -u_x^2 + \frac{P_{xx}}{\rho} & 2u_x & 0 & 0 & 0 & 0 & 0 \\
0 & 0 & 0 & 0 & 0 & 0 & 1 & 0 & 0 & 0 \\
u_x^2 u_z - \frac{P_{xx}u_z}{\rho} - \frac{2P_{xz}u_x}{\rho} & -2u_x u_z + \frac{2P_{xz}}{\rho} & u_z & 0 & 0 & -u_x^2 + \frac{P_{xx}}{\rho} & 2u_x & 0 & 0 & 0 \\
u_x u_y^2 - \frac{P_{yy}u_x}{\rho} - \frac{2P_{xy}u_y}{\rho} & -u_y^2 + \frac{P_{yy}}{\rho} & 0 & -2u_x u_y + \frac{2P_{xy}}{\rho} & 2u_y & 0 & 0 & u_x & 0 & 0 \\
u_x u_y u_z - \frac{P_{yz}u_x}{\rho} - \frac{P_{xz}u_y}{\rho} - \frac{P_{xy}u_z}{\rho} & -u_y u_z + \frac{P_{yz}}{\rho} & 0 & -u_x u_z + \frac{P_{xz}}{\rho} & u_z & -u_x u_y + \frac{P_{xy}}{\rho} & u_y & 0 & u_x & 0 \\
u_x u_z^2 - \frac{P_{zz}u_x}{\rho} - \frac{2P_{xz}u_z}{\rho} & -u_z^2 + \frac{P_{zz}}{\rho} & 0 & 0 & 0 & -2u_x u_z + \frac{2P_{xz}}{\rho} & 2u_z & 0 & 0 & u_x
\end{bmatrix}
$$

- Block diagonal structure also breaks up the characteristic polynomial:

$$
\det\left(\lambda I - \frac{\partial \boldsymbol{F}_x}{\partial \boldsymbol{U}}\right) = He_3\left(\sqrt{\frac{\rho}{P_{xx}}}(\lambda - u_x)\right) \cdot He_2^2\left(\sqrt{\frac{\rho}{P_{xx}}}(\lambda - u_x)\right) \cdot He_1^3\left(\sqrt{\frac{\rho}{P_{xx}}}(\lambda - u_x)\right) = 0
$$

10-Moment Flux Jacobian

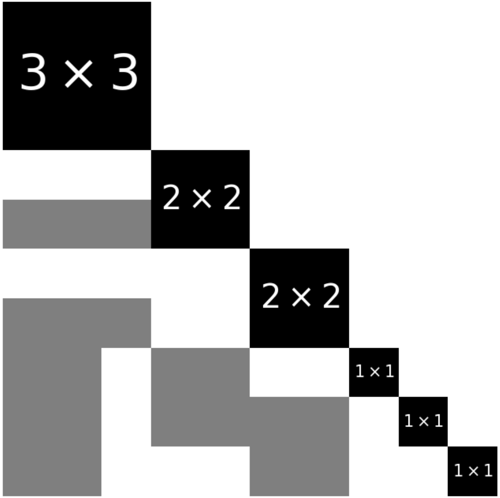

20-Moment Equations

- Continuity Equation:

$$\frac{\partial}{\partial t}(\rho) + \frac{\partial}{\partial x_i}(\rho u_i) = 0$$

- Momentum Equation:

$$\frac{\partial}{\partial t}(\rho u_i) + \frac{\partial}{\partial x_j}(\rho u_i u_j + P_{ij}) = 0$$

- Energy Equation:

$$\frac{\partial}{\partial t}(\rho u_i u_j + P_{ij}) + \frac{\partial}{\partial x_k}(\rho u_i u_j u_k + P_{ij} u_k + P_{ik} u_j + P_{jk} u_i + Q_{ijk}) = \boldsymbol{S}(\boldsymbol{U})$$

- Heat Flux Equation:

$$\frac{\partial}{\partial t}(\rho u_i u_j u_k + P_{ij} u_k + P_{ik} u_j + P_{jk} u_i + Q_{ijk}) + \frac{\partial}{\partial x_l}(\rho u_i u_j u_k u_l + P_{ij} u_k u_l + P_{ik} u_j u_l + P_{jk} u_i u_l$$
$$+ P_{il} u_j u_k + P_{jl} u_i u_k + P_{kl} u_i u_j + Q_{ijk} u_l + Q_{ijl} u_k + Q_{ikl} u_j + Q_{jkl} u_i + R_{ijkl}) = \boldsymbol{S}(\boldsymbol{U})$$

Technique for Extending High Order Closures to Multidimensional Gases

- What if you build similar flux Jacobians for higher-order, non-equilibrium systems but with the same block diagonal structure?
- Requirements:
  1. Flux Jacobian must have real eigenvalues
  2. Convected moments should be Galilean invariant
- Variables for a 20-moment closure:
  1. Scalar ρ for density
  2. Vector u_i with 3 entries for velocity
  3. General pressure tensor P_{ij} with 6 entries
  4. General heat flux tensor Q_{ijk} with 10 entries
  5. Full tensor R_{ijkl} has 15 entries (10 of which close system of 20 known moments per direction)

20-Moment Closure Construction

- Begin by prescribing the desired one-dimensional closures for each subsystem block along the main diagonal

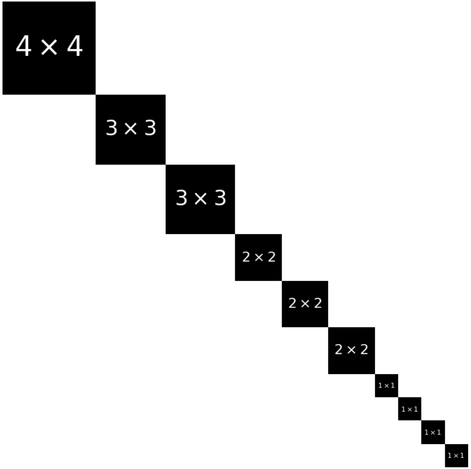

20-Moment Closure Construction

- Begin by prescribing the desired one-dimensional closures for each subsystem block along the main diagonal
- Lower triangle elements can be used to get the correct convected form of the moments without spoiling hyperbolicity

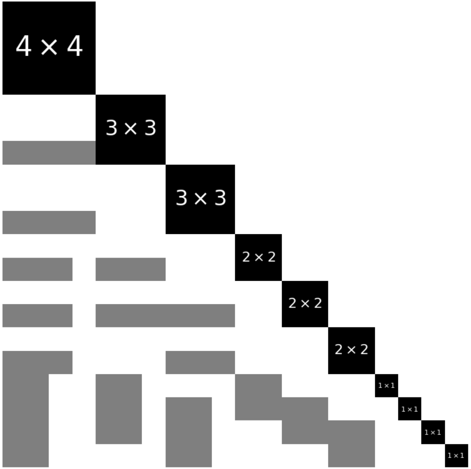

20-Moment Closure Construction

- Begin by prescribing the desired one-dimensional closures for each subsystem block along the main diagonal
- Lower triangle elements can be used to get the correct convected form of the moments without spoiling hyperbolicity
- Symmetries between $\frac{\partial \boldsymbol{F}_x}{\partial \boldsymbol{U}}$, $\frac{\partial \boldsymbol{F}_y}{\partial \boldsymbol{U}}$ and $\frac{\partial \boldsymbol{F}_z}{\partial \boldsymbol{U}}$ can further be imposed to improve rotational properties

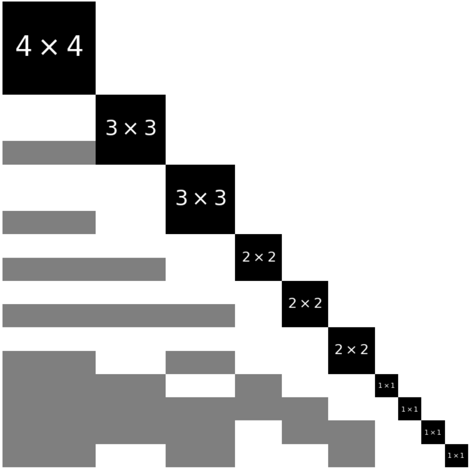

20-Moment Closing Fluxes

- Closing R_{ijkl} which are robustly hyperbolic, and symmetric between Jacobians in each direction

$$R_{xxxx} = 2\frac{Q_{xxx}^2}{P_{xx}} + 3\frac{P_{xx}^2}{\rho} \qquad R_{yyyy} = 2\frac{Q_{yyy}^2}{P_{yy}} + 3\frac{P_{yy}^2}{\rho} \qquad R_{zzzz} = 2\frac{Q_{zzz}^2}{P_{zz}} + 3\frac{P_{zz}^2}{\rho}$$

$$R_{xxxy} = 2\frac{Q_{xxx}Q_{xxy}}{P_{xx}} + 3\frac{P_{xx}P_{xy}}{\rho} \qquad R_{xxxz} = 2\frac{Q_{xxx}Q_{xxz}}{P_{xx}} + 3\frac{P_{xx}P_{xz}}{\rho} \qquad R_{xyyy} = 2\frac{Q_{xyy}Q_{yyy}}{P_{yy}} + 3\frac{P_{xy}P_{yy}}{\rho}$$

$$R_{xzzz} = 2\frac{Q_{zzz}Q_{xzz}}{P_{zz}} + 3\frac{P_{xz}P_{zz}}{\rho} \qquad R_{yyyz} = 2\frac{Q_{yyy}Q_{yyz}}{P_{yy}} + 3\frac{P_{yy}P_{yz}}{\rho} \qquad R_{yzzz} = 2\frac{Q_{zzz}Q_{yzz}}{P_{zz}} + 3\frac{P_{yz}P_{zz}}{\rho}$$

$$R_{xxyy} = \frac{Q_{xxy}^2}{P_{xx}} + \frac{Q_{xyy}^2}{P_{yy}} + 2\frac{P_{xy}^2}{\rho} + \frac{P_{xx}P_{yy}}{\rho} \qquad R_{xxzz} = \frac{Q_{xxz}^2}{P_{xx}} + \frac{Q_{xzz}^2}{P_{zz}} + 2\frac{P_{xz}^2}{\rho} + \frac{P_{xx}P_{zz}}{\rho}$$

$$R_{yyzz} = \frac{Q_{yyz}^2}{P_{yy}} + \frac{Q_{yzz}^2}{P_{zz}} + 2\frac{P_{yz}^2}{\rho} + \frac{P_{yy}P_{zz}}{\rho}$$

$$R_{xxyz} = \frac{Q_{xxy}Q_{xxz}}{P_{xx}} + \frac{Q_{xxx}Q_{xyz}}{P_{xx}} + \frac{P_{xx}P_{yz}}{\rho} + 2\frac{P_{xy}P_{xz}}{\rho} \qquad R_{xyyz} = \frac{Q_{xyy}Q_{yyz}}{P_{yy}} + \frac{Q_{yyy}Q_{xyz}}{P_{yy}} + \frac{P_{xz}P_{yy}}{\rho} + 2\frac{P_{xy}P_{yz}}{\rho}$$

$$R_{xyzz} = \frac{Q_{yzz}Q_{xzz}}{P_{zz}} + \frac{Q_{zzz}Q_{xyz}}{P_{zz}} + \frac{P_{xy}P_{zz}}{\rho} + 2\frac{P_{xz}P_{yz}}{\rho}$$

Multidimensional Riemann Problem

- Similar to a classic Sod shock tube, bubble of high density and pressure but same temperature as surroundings
- Study the model's structure in three regimes:
  1. Continuum, particle collisions fully relax moment methods to Euler solutions
  2. Transition, moderate particle collisions and regime of highest interest for moment methods
  3. Free Molecular, no particle collisions and shows mathematical structure of PDEs

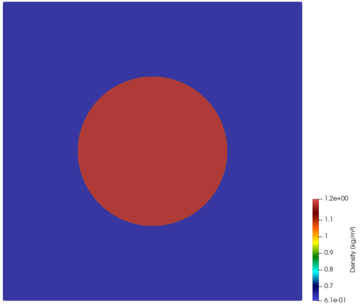

Multidimensional Riemann Problem

- 20-Moment continuum solution matches Euler

Continuum Density ρ

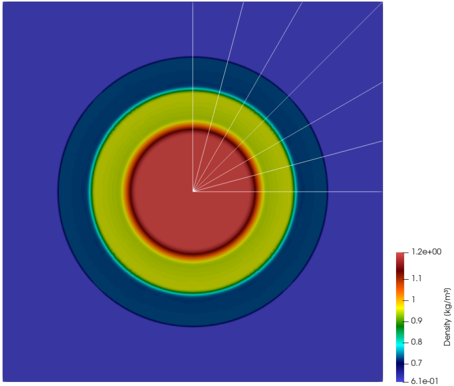

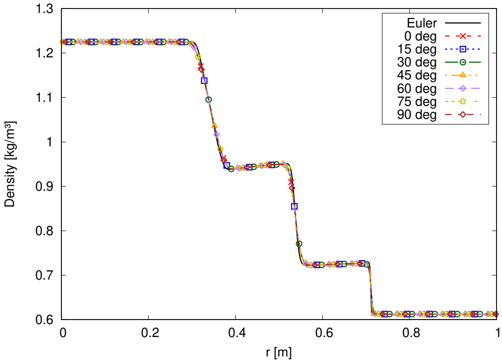

Multidimensional Riemann Problem

- Heat flux inside waves can be captured

Continuum Radial Heat Flux Q_{rrr}

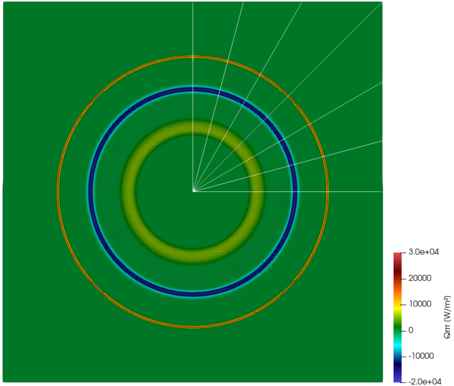

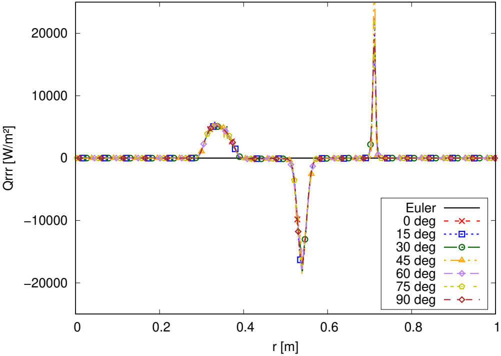

Multidimensional Riemann Problem

- 20-moment transition solution also agrees with expensive BGK solution

Transition Density ρ

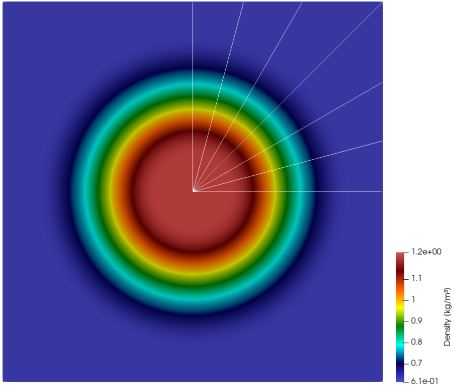

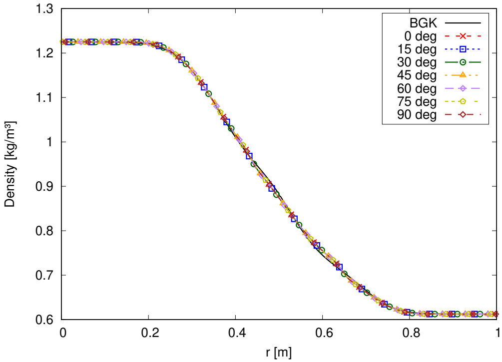

Multidimensional Riemann Problem

- Heat flux throughout the domain is captured very well

Transition Radial Heat Flux Q_{rrr}

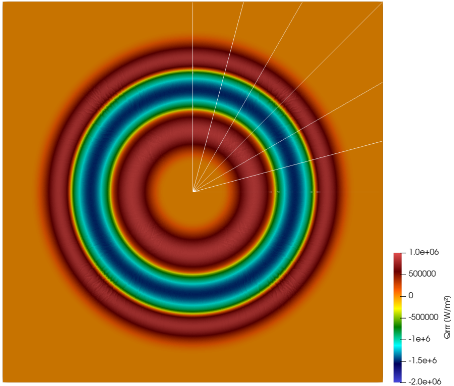

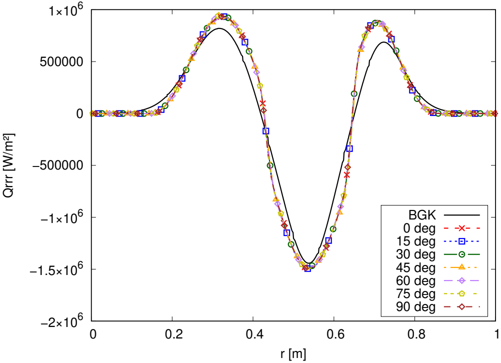

Multidimensional Riemann Problem

- Free molecular no longer agrees with BGK, but has expected differences

Free Molecular Density ρ

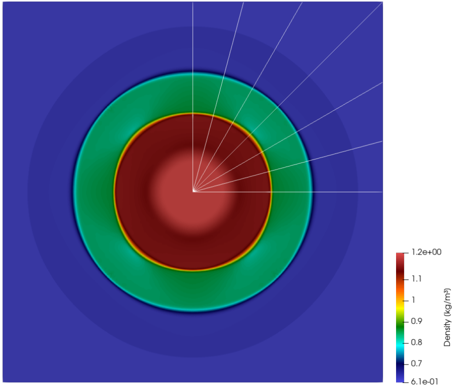

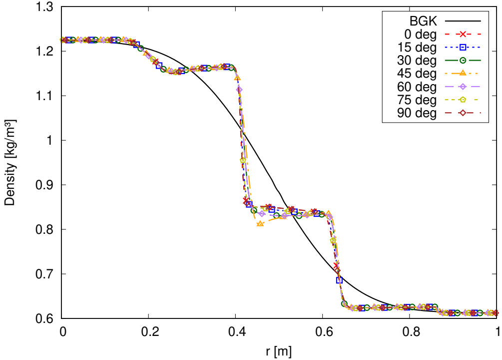

Multidimensional Riemann Problem

- Free molecular no longer agrees with BGK, but has expected differences

Free Molecular Radial Heat Flux Q_{rrr}

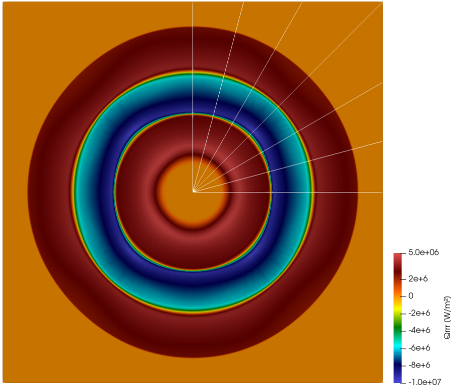

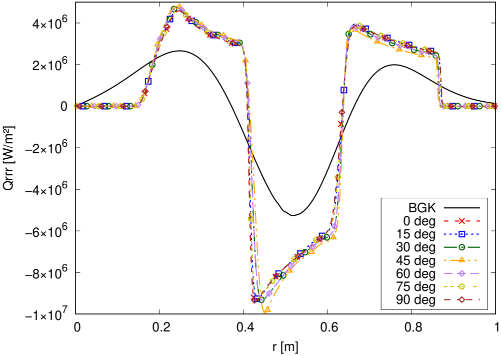

Mach 8 Shock Profiles for a Realistic 3D Gas

- Non-equilibrium throughout the shock is accurately captured
- Temperature anisotropies can be efficiently resolved

Density ρ

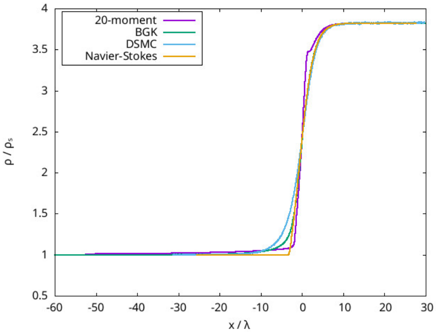

Normal Heat Flux Q^*_{xii}

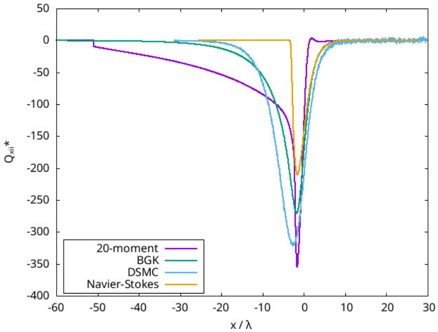

Mach 8 Shock Profiles for a Realistic 3D Gas

- Non-equilibrium throughout the shock is accurately captured
- Temperature anisotropies can be efficiently resolved

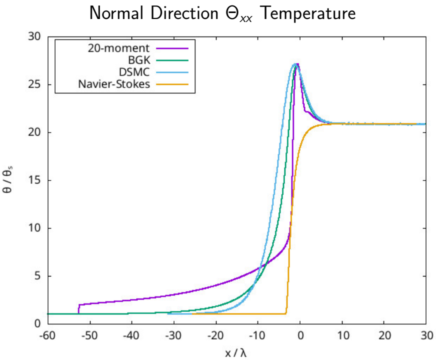

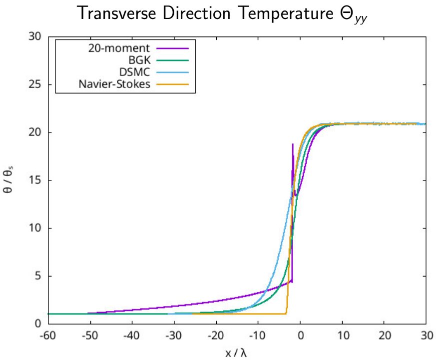

Hypersonic Flow Past a Plate, Mach 8, Kn = 0.1, (Boccelli et al. 2023)

20-Moment versus DSMC Density

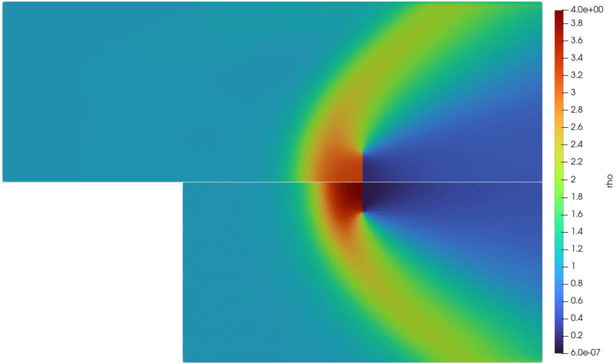

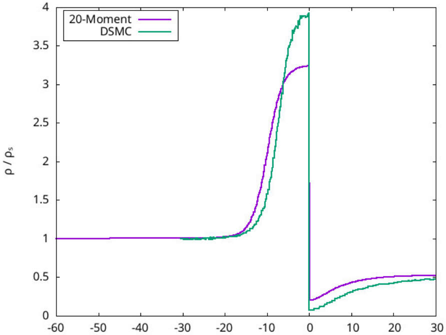

Hypersonic Flow Past a Plate, Mach 8, Kn = 0.1, (Boccelli et al. 2023)

20-Moment versus DSMC Temperature Anisotropy

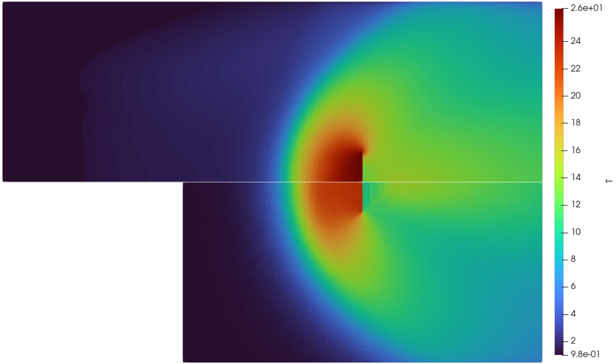

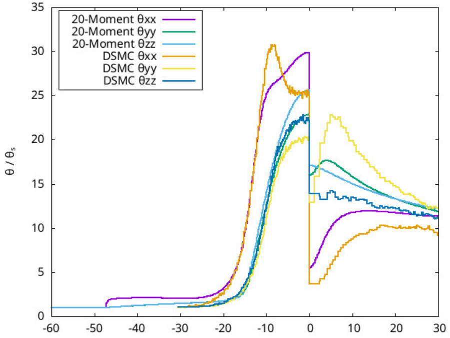

Hypersonic Flow Past a Plate, Mach 8, Kn $= 0.1$, (Boccelli et al. 2023)

20-Moment versus DSMC Heat Flux

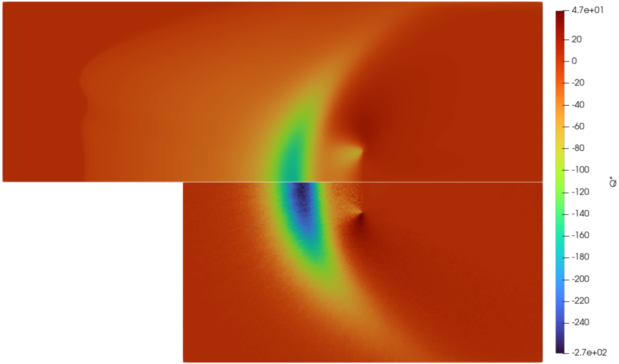

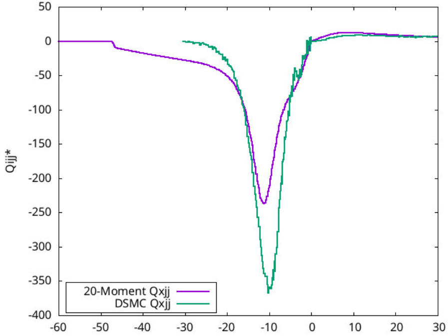

Double Mach Reflection (Deschambault and Glass, 1982)

- Incoming shock wave encounters wedge

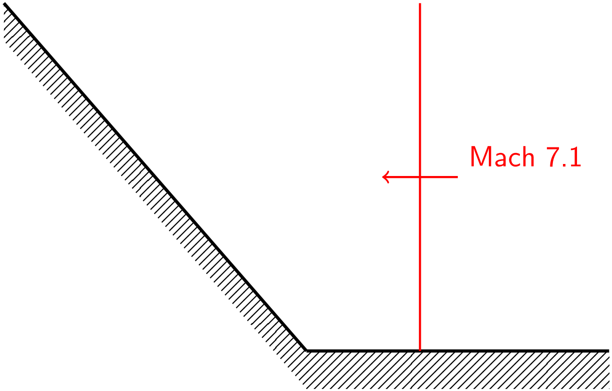

Double Mach Reflection (Deschambault and Glass, 1982)

- Incoming shock wave encounters wedge
- Interaction results in similar shock structures that are seen in detonations, but for an inert gas

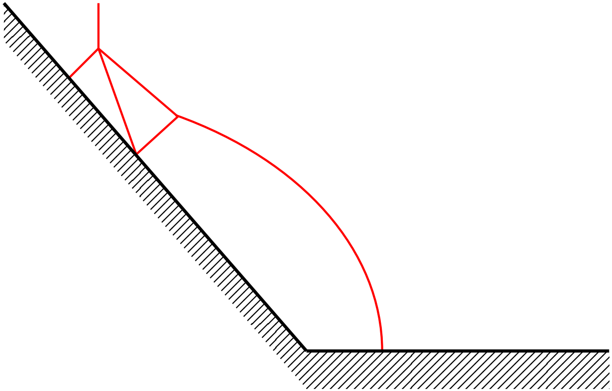

Double Mach Reflection (Deschambault and Glass, 1982)

Experimental Density

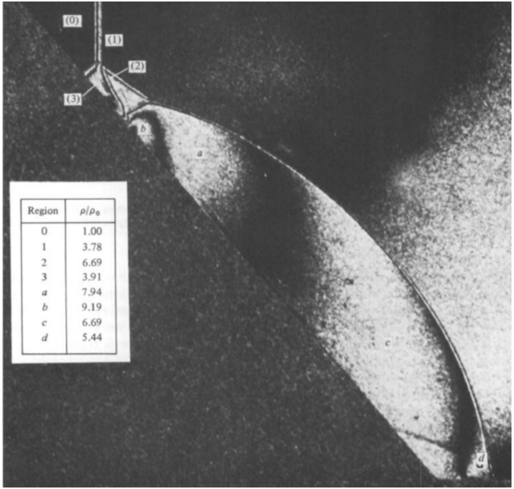

Region	ρ/ρ_0
0	1.00
1	3.78
2	6.69
3	3.91
a	7.94
b	9.19
c	6.69
d	5.44

20-Moment Density

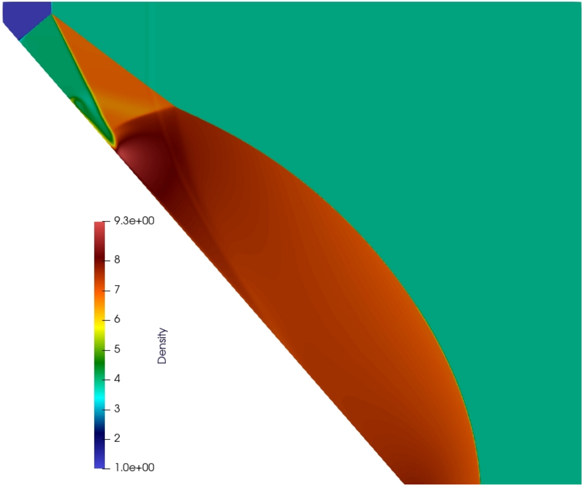

Non-Equilibrium in Double Mach Reflections

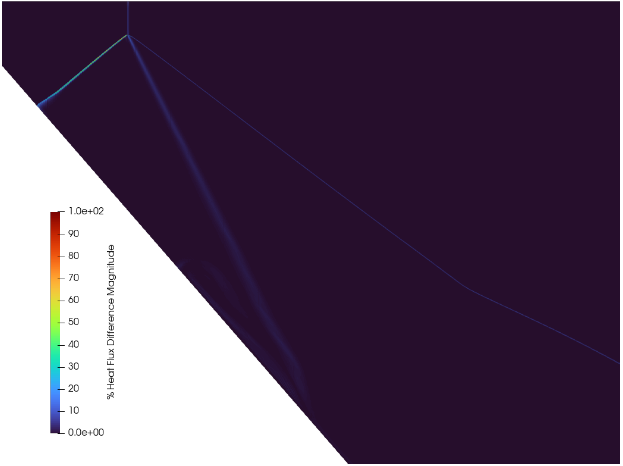

- Difference between 20-moment model and Fourier's Law is significant

$$\left| \frac{1}{2} Q_{ijj} - k \nabla T \right| > 0$$

- Temperature at the triple point is highly anisotropic

$$\kappa \left(T_{ij} \right) \approx 3$$

Conclusion

- The new hierarchy of moment methods can capture non-equilibrium effects present in strong shocks which are otherwise invisible or expensive for traditional methods
- Model can be made more sophisticated to account for rotational and vibrational energy modes of larger molecules
- Comparison between new model and DSMC for other Knudsen number regimes in the works
- Realistic solid-wall boundary conditions in development

Thank you!